In Vivo Autofluorescence Spectroscopy of Oral Premalignant and Malignant Lesions: Distortion of Fluorescence Intensity by Submucous Fibrosis

Tsuimin Tsai, PhD,[1] Hsin-Ming Chen, BDS, MS,[2] Chih-Yu Wang, PhD,[3] Jui-Chang Tsai, MD, PhD,[4] Chin-Tin Chen, PhD,[5]* and Chun-Pin Chiang, BDS, DMSc[6]

[1]*Graduate Institute of Biomedical Materials, Taipei Medical University, Taipei, Taiwan*
[2]*Graduate Institute of Clinical Dentistry, Taipei Medical University, Taipei, Taiwan*
[3]*Department of Biomedical Engineering, I-Shou University, Taiwan*
[4]*Department of Neurosurgery & Center for Optoelectronic Biomedicine, Taipei, Taiwan*
[5]*Center for Optoelectronic Biomedicine & Graduate Institute of Oral Biology, Taipei, Taiwan*
[6]*School of Dentistry, College of Medicine, National Taiwan University, Taipei, Taiwan*

Background and Objectives: To test whether autofluorescence spectroscopy can be used for the diagnosis of oral neoplasia in a high-risk population, we characterized the in vivo autofluorescence spectra from oral submucous fibrosis (OSF) lesions and oral premalignant and malignant lesions in both OSF and non-OSF patients.

Study Design/Materials and Methods: Autofluorescence emission spectra were measured under the excitation wavelength of 330 nm, using a Xenon lamp-based fluorospectrometer coupled to a handheld optical fiber probe. Autofluorescence spectroscopies were analyzed among patients with OSF lesions, and oral lesions of epithelial hyperkeratosis (EH), epithelial dysplasia (ED), and squamous cell carcinomas (SCC) and normal oral mucosa (NOM) of healthy volunteers.

Results: We found that the most intensely autofluorescence emission peaks occurred at 380 nm and 460 nm. For comparing the spectral patterns among different groups of oral lesions and NOM, ratios of the area under the spectrum of 460 ± 10 nm to that under the spectrum of 380 ± 10 nm (denoted as $A_{460 \pm 10\,nm}/A_{380 \pm 10\,nm}$) were calculated. The mean ratio values increased gradually from OSF to NOM, to EH and ED, and to SCC. The ANOVA test showed significant differences in the ratio value among all categories of samples ($P < 0.01$). On the other hand, we found that EH, ED, and SCC lesions on OSF patients had distorted autofluorescence intensity. The mean ratio values of EH, ED, and SCC between non-OSF and OSF patients show significant differences. Furthermore, an ANOVA test showed NOM is not distinguishable from EH and ED lesions on oral fibrotic mucosa ($P > 0.05$).

Conclusions: Autofluorescence spectroscopy can be used to diagnose EH, ED, and SCC lesions in non-OSF patients but not in OSF patients. Lasers Surg. Med. 33:40–47, 2003.

Key words: fluorescence spectroscopy; oral neoplasia; oral submucous fibrosis

INTRODUCTION

In Taiwan, oral cancer is among the ten most common malignancies. Its prevalence is increasing every year due to the popular areca quid (AQ) chewing habit [1]. Presently, there are more than 2.3 million people who have this AQ chewing habit. This AQ chewing habit causes many clinical cases of oral submucous fibrosis (OSF), oral leukoplakia, and oral squamous cell carcinoma (SCC). In fact, over the past decade, the numbers of death from oral cancers has been doubled. According to the cancer registry annual report published by the Department of Health, Taiwan, oral cancers showed the highest annual rate of increase among male patients in 2001. Presently, there are more than 2.3 million people who have this AQ chewing habit and approximately 80% of all oral cancer deaths are associated with this habit [2,3]. This AQ chewing habit causes oral submucous fibrosis (OSF), oral leukoplakia, and oral squamous cell carcinoma (SCC). Oral cancer has one of the lowest 5-year survival rates among the major cancers. For advanced cases, the 5-year oral cancer survival rate is 18%, compared with 76% for localized lesions [4]. In this regard, early diagnosis can provide more effective treatment of this lethal disease. The most common symptoms and signs of early oral neoplastic lesions are painless tumors, long-standing ulcers, or thickening of the oral

Chin-Tin Chen and Chun-Pin Chiang contributed equally to this study.

Contract grant sponsor: National Science Council, Taipei, Taiwan (Research Grants); Contract grant numbers: NSC 89-2736-L-038-001, NSC90-2736-L-002-004.

*Correspondence to: Dr. Chin-Tin Chen, PhD, Center for Optoelectronic Biomedicine, College of Medicine, National Taiwan University, No. 1, Jen-Ai Road, Sec. 1, Taipei 100, Taiwan.
E-mail: ctchen@ha.mc.ntu.edu.tw

Accepted 12 March 2003
Published online in Wiley InterScience (www.interscience.wiley.com).
DOI 10.1002/lsm.10180

mucosa. Early oral neoplastic lesions are difficult to differentiate from innocuous tissues; therefore, the early stages of neoplasia are often neglected. Presently, incisional biopsy remains the most reliable diagnostic method for the detection of oral neoplasia. However, even an experienced clinician cannot easily choose a representative and proper site on a large oral premalignant or malignant lesion for biopsy. Therefore, development of a simple, noninvasive diagnostic tool that can detect oral neoplasia in the early stage would be important for these high-risk AQ-chewing patients.

Autofluorescence spectroscopy has shown promising results in differentiating normal from neoplastic tissues. The principle of autofluorescence spectroscopy is based on the fact that different diseased tissues contain different morphohistological characteristics and intrinsic fluorophores that give rise to different fluorescence emission spectra when the tissues are excited at a suitable wavelength [5]. This technique has been used to detect neoplastic tissues in a variety of organ systems, such as the cervix of uterus, colorectum, lungs, and head and neck [6–10]. These studies suggest the possibility of using autofluorescence spectroscopy in cancer diagnosis.

For effective management of oral neoplasia, we have previously shown that autofluorescence spectroscopy can be used to differentiate oral neoplastic tissue from normal tissue in patients with AQ-chewing habit in ex vivo studies [11,12]. Under 330-nm excitation wavelength, significant differences in fluorescence intensity between human oral malignant and normal tissues were observed around the 380-nm and 460-nm emission [11]. Using a DMBA-induced hamster buccal pouch carcinogenesis model, we further demonstrated that the changes in fluorescence intensity were correlated with the progressive development of DMBA-induced buccal pouch cancer [12]. To examine whether autofluorescence spectroscopy can be used for the diagnosis of oral neoplasia in a high-risk population, we further characterized the in vivo autofluorescence spectra from OSF lesions and different groups of oral lesions of epithelial hyperkeratosis (EH), epithelial dysplasia (ED), and SCC in both OSF and non-OSF patients. As autofluorescence intensity of EH, ED, and SCC lesions was distorted by fibrotic mucosa, we found that autofluorescence spectroscopy is only suitable for diagnosis of EH, ED, and SCC lesions in non-OSF patients but not in OSF patients.

MATERIALS AND METHODS

Study Group

Fifteen healthy volunteers and 149 patients with clinically suspected OSF, EH, ED, and SCC oral mucosal lesions were recruited from the Department of Oral and Maxillofacial Surgery, National Taiwan University Hospital. This study was reviewed and approved by the Human Investigation Review Committee at the National Taiwan University Hospital. All the patients had AQ chewing habits and the examined tissues of this study were at the location of oral buccal mucosa. After in vivo spectroscopic measurements, biopsy specimens (except for healthy volunteers) were taken from the oral lesions for which fluorescence spectra were measured. The taken specimens were fixed in 10% neutral formalin, embedded, sectioned, and stained with hematoxylin and eosin. An oral pathologist who was blinded to the fluorescence spectral results performed all histopathological assessments in another laboratory.

Fluorescence Instrument and In Vivo Autofluorescence Measurement

Fluorescence excitation–emission spectra were measured from each sample using a handheld optical fiber probe attached to a spectrofluorometer (SkinSkan, JC, Urbana, IL). A monochromator with a 150 W ozone-free Xenon lamp provides the excitation light. The desired excitation wavelength and the emission spectrum were selected by motor-controlled monochromators. The excitation light was guided to illuminate samples by one arm of a Y-type quartz fiber bundle, and the emission fluorescence was collected by another arm of the fiber bundle. The tip of the fiber bundle was specially designed in a bent shape to be convenient for measurements in the oral cavity. After the oral cavity of patient was examined and cleaned, the tip of the fiber bundle was gently placed on the selected site of the buccal mucosa, and the measurement started. The measurement took 30 seconds. The optical fiber probe was disinfected with 2.4% glutaraldehyde solution before each clinical use.

The excitation wavelength was chosen to be 330 nm, because it has been shown that the band around this wavelength (320–340 nm) can distinguish normal from abnormal human tissues with the best efficiency [11–14]. The emission spectrum of autofluorescence was measured at wavelengths ranging from 340 to 601 nm in 3-nm increments. To avoid the possible effects of photobleaching, we processed two measurements from each sample. It was found that differences between the two spectra obtained from the two measurements were less than 2%, which showed that no photobleaching occurred. To avoid intensity alterations due to variations in excitation light power and fluorescence collection efficiency, all obtained spectra were normalized by dividing the intensity of each wavelength by the integrated area under the total emission spectrum.

RESULTS

Comparison Among NOM, OSF Lesions, and EH, ED, and SCC Lesions in Non-OSF Patients

Figure 1A shows the average normalized fluorescence spectra obtained from NOM, OSF lesions, and oral lesions of EH, ED, and SCC in non-OSF patients at 330-nm excitation. The most intense peaks of the autofluorescence spectra occurred around the 380- and 460-nm emissions in all samples measured. It was important to note that while the emission peaks of each individual might have varied, they still occurred within ± 10 nm of 380 and 460 nm. The OSF samples had the highest intensity of the 380-nm emission peak, followed by NOM, EH or ED, and SCC samples in a descending order. In contrast, SCC samples

had the strongest intensity of 460 nm emission peak, followed by the EH or ED, NOM, and OSF samples in a descending order. To rule out the possible individual-to-individual variation in intensity and to quantify the

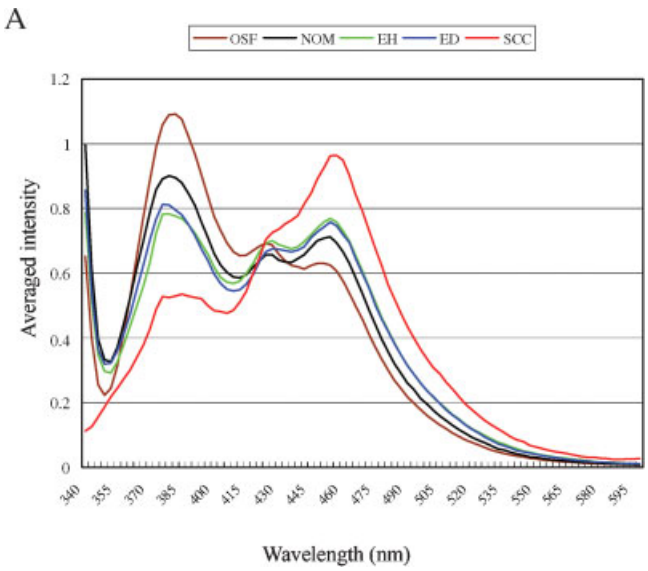

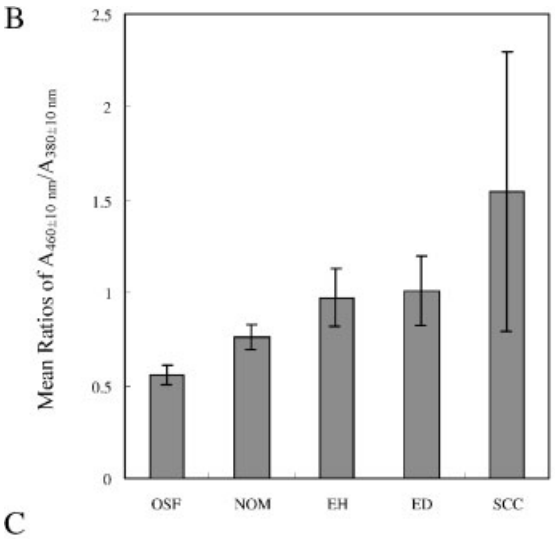

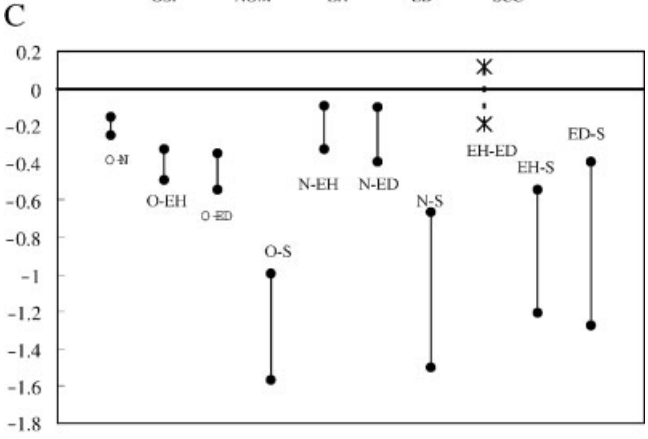

Fig. 1. **A**: Normalized averaged fluorescence emission spectra obtained from 15 volunteers of normal oral mucosa (NOM), 30 patients of oral submucous fibrosis (OSF), and 25 patients of epithelial hyperkeratosis (EH), 15 patients of epithelial dysplasia (ED), and 13 patients of squamous cell carcinoma (SCC) in non-OSF patients. Fluorescence intensities are reported in calibrated units. **B**: A histogram of the mean ratios of $A_{460\pm10\ nm}/A_{380\pm10\ nm}$ for NOM, OSF lesions, and oral EH, ED, and SCC lesions in non-OSF patients. The error bars are standard deviations. **C**: Multiple comparisons among five categories of samples with different pathological characteristics. Notation: O, oral submucous fibrosis (OSF); N, normal oral mucosa (NOM); EH, epithelial hyperkeratosis; ED, epithelial dysplasia; and S, squamous cell carcinoma (SCC).

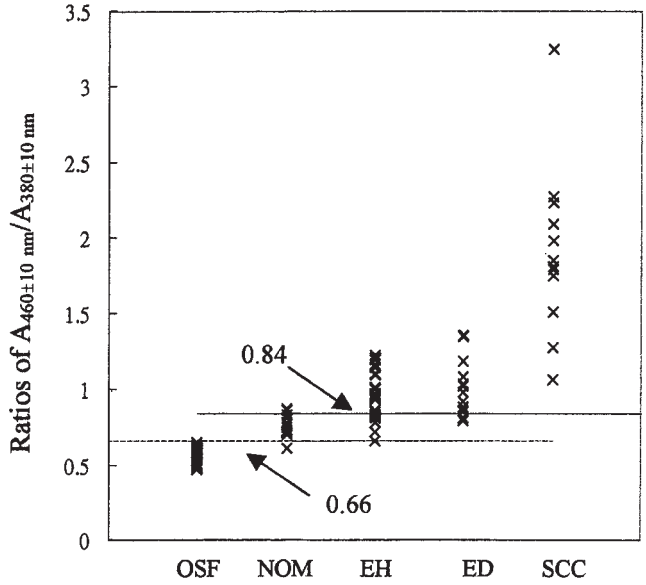

Fig. 2. Scattering plot for NOM, OSF lesions, and oral EH, ED, and SCC lesions in non-OSF patients with two classification thresholds.

alterations in the spectral profile, a simple algorithm based on the ratio of the area under the spectrum of 460 ± 10 nm to that under the spectrum of 380 ± 10 nm ($A_{460\pm10\ nm}/A_{380\pm10\ nm}$) was performed. Although innocuous normal tissues from the same patients were used for comparison in other studies [9,10], we found considerable overlap in the ratios of $A_{460\pm10\ nm}/A_{380\pm10\ nm}$ between clinically suspicious lesions and their corresponding contralateral normal mucosal tissues in individual AQ-chewing patients (data not shown). In this regard, normal mucosal tissues from healthy volunteers but not from same individuals were compared in this study. The ratios of $A_{460\pm10\ nm}/A_{380\pm10\ nm}$ for NOM ranged from 0.61 to 0.87 while that for OSF lesions ranged from 0.46 to 0.64. The ratio scores for the 25 EH lesions distributed from 0.66 to 1.23, which had a marked overlap with the ratio range of 0.79 to 1.36 for the

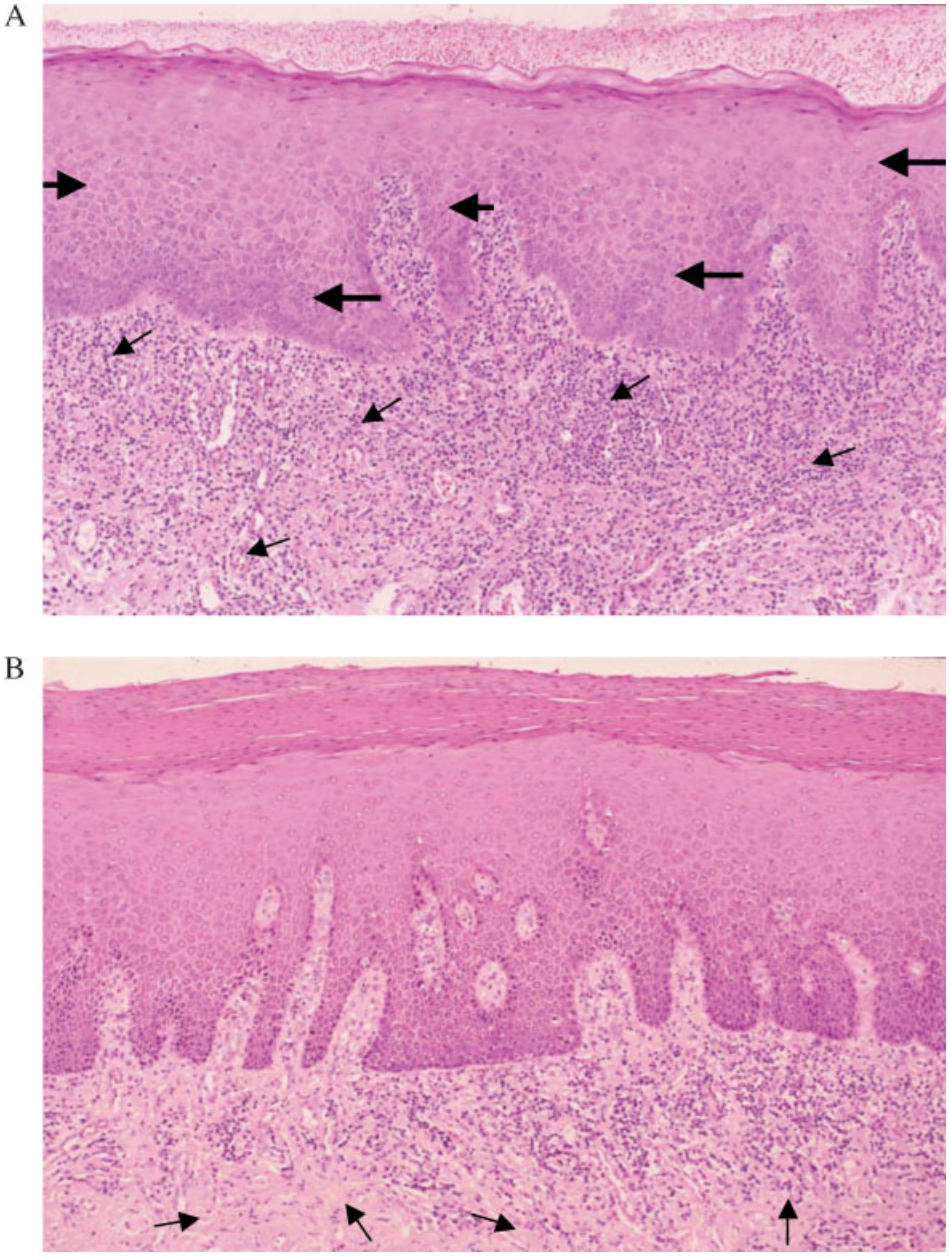

Fig. 3. **A**: A specimen taken from buccal mucosa showing moderate epithelial dysplasia (area indicated by thick arrows) and a marked lymphoplasma cell infiltrate in the lamina propria (indicated by thin arrows). **B**: A specimen taken from buccal mucosa showing moderate epithelial dysplasia as well as a moderate lymphoplasma cell infiltrate and marked fibrosis (indicated by thin arrows) in the lamina propria.

15 ED lesions. However, the ratio of $A_{460\pm10\ nm}/A_{380\pm10\ nm}$ for the 13 SCC lesions ranging from 1.06 to 3.25 was significantly higher than those for OSF, EH and ED lesions and for NOM. As shown in Figure 1B, the histograms of the mean ratios gradually increased from OSF to NOM, to EH or ED, and to SCC samples. An ANOVA test showed significant differences in values of the ratio among all categories of samples ($P < 0.01$).

To further identify the relationship between groups, a multiple comparisons method, which is a technique for comparing more than 3 categories by drawing their $100(1-\alpha)\%$ confidence interval [15], was employed to show the 99% confidence interval of mean differences between any two groups. The principle of "multiple comparisons" is to evaluate the population means of any two groups (denoted as μ_g and μ_h, $g \neq h$). The lower bound (L) and

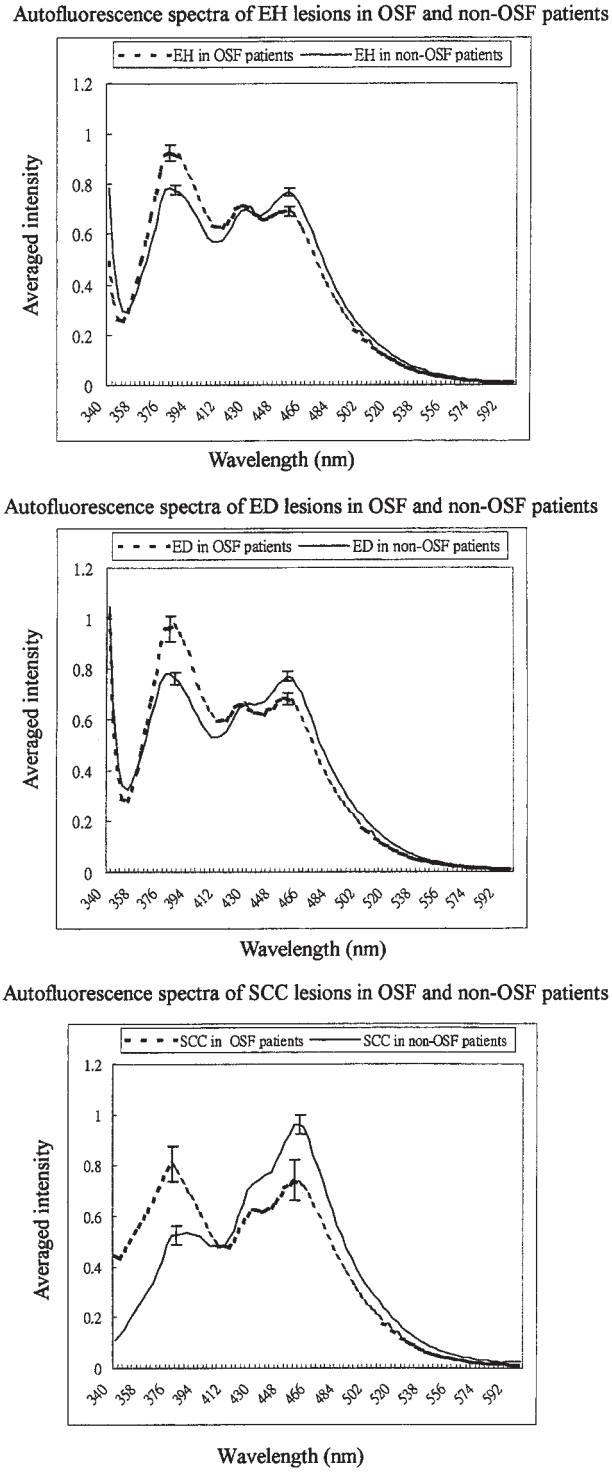

Fig. 4. **A**: Normalized averaged autofluorescence spectra of EH lesions on OSF (n = 32) and non-OSF (n = 25) patients; **B**: normalized averaged autofluorescence spectra of ED lesions on OSF (n = 12) and non-OSF (n = 15) patients; **C**: normalized averaged autofluorescence spectra of SCC lesions on OSF (n = 7) and non-OSF (n = 13) patients. Fluorescence intensities are reported in calibrated units.

upper bound (U) for the 100(1−α)% confidence interval of ($\mu_g - \mu_h$) is represented as:

$$L = (\overline{X}_g - \overline{X}_h) - t_{\frac{\alpha}{2}} S_p \sqrt{\frac{1}{n_g} + \frac{1}{n_k}},$$

$$U = (\overline{X}_g - \overline{X}_h) - t_{\frac{\alpha}{2}} S_p \sqrt{\frac{1}{n_g} + \frac{1}{n_h}},$$

where $\overline{X}_g$ and $\overline{X}_h$ are the sample means of categories g and h, respectively; S_p^2 stands for the pooled sample variance; n_g and n_h are the sample sizes. If the range (L, U) contains the origin, the mean difference ($\mu_g - \mu_h$) may equal to zero under (1−α) significant level. If $L > 0$ (or $U < 0$), the mean difference ($\mu_g - \mu_h$) may be positive (or negative) under (1−α) significant level. Figure 1C shows that only the confidence interval of EH and ED contains the origin, indicating that $\mu_{OSF} < \mu_{NOM} < \mu_{EH} = \mu_{ED} < \mu_{SCC}$, where μ represents the mean value. Therefore, it is possible to develop a diagnostic algorithm for the NOM and OSF, EH, ED, and SCC lesions by using the autofluorescence spectroscopy in spite of the fact that the diagnostic algorithm could not differentiate EH from ED.

To quantitatively evaluate the discriminated ability of our algorithm, a receiver operating characteristic (ROC) curve was used. The ROC curve is a graphic method, which helps us speculate on the relationship between specificity and sensitivity under various thresholds that distinguish two populations. The false positive rate (1 − specificity) and the sensitivity are plotted on a two-dimension scatter plot under various threshold values [16]. A diagnostic algorithm with ROC curve located near the upper left corner of the plot, at which both the specificity and sensitivity are high, are normally considered as effective. The curve is thus helpful for determining the threshold for some desired specificity and sensitivity. We apply ROC curves with threshold varying from 0 to 3 in 0.01 steps. Figure 2 shows the scattering plot of OSF, NOM, EH, ED, and SCC samples, with thresholds described below. In viewing the separation of NOM and OSF, we found that the optimal sensitivity and specificity are 100% and 93%, respectively, when the threshold value was set to be 0.66. On the other hand, by focusing on the division between NOM and premalignant (EH and ED) or malignant tissues (SCC), it was observed that the optimal sensitivity and specificity are 81% and 87%, respectively, when the threshold value was set to be 0.84.

Fluorescence Spectra Analysis of EH, ED, and SCC Lesions in OSF Patients

In Taiwan, because of the AQ chewing habit, EH, ED, and SCC lesions are frequently found in OSF patients. Figure 3 shows the representative histologies of the dysplasia lesions in non-OSF and OSF patients. As shown in Figure 3B, compared to pure epithelial dysplasia, a marked fibrosis in the lamina propria could be found below the dysplastic epithelium. To assess the influence of tissue fibrosis on the fluorescence emission of EH, ED, and SCC

TABLE 1. Mean Ratios of $A_{460\pm10\ nm}/A_{380\pm10\ nm}$ for Epithelial Dysplasia (ED), Epithelial Hyperkeratosis (EH), and Squamous Cell Carcinoma (SCC) Samples in Oral Submucous Fibrosis (OSF) Patients and Non-OSF Patients as Well as Unpaired Student's *t*-Test Results

Pathological characteristics	Patient no.	Average intensity ratio ± standard deviation	Unpaired Student's *t*-test between lesions with or without OSF
HYP	25	0.97 ± 0.17	$P < 0.001$
HYP with OSF	32	0.77 ± 0.26	
DYS	15	1.01 ± 0.19	$P < 0.001$
DYS with OSF	12	0.68 ± 0.22	
SCC	13	1.54 ± 0.75	$P < 0.005$
SCC with OSF	7	1.25 ± 0.77	

lesions, we further examined the autofluorescence spectra of EH, ED, and SCC lesions occurring in OSF patients. As shown in Figure 4, we found that the intensity of emission peak around 380 nm for EH, ED, or SCC lesions in OSF patients was significantly higher than that for corresponding lesions in non-OSF patients. However, the intensity of emission peaks around 460 nm for EH, ED, or SCC lesions in OSF patients was significantly lower than that for corresponding lesions in non-OSF patients. As shown in Table 1, a significant difference in the mean ratio of $A_{460\pm10\ nm}/A_{380\pm10\ nm}$ was found between oral EH, ED, or SCC lesions in OSF patients and those corresponding lesions in non-OSF patients ($P < 0.05$ by unpaired Student's *t*-test). These results suggest that underlying tissue fibrosis, as shown in Figure 3B, might interfere with the fluorescence emissions of premalignant or malignant lesions on the fibrotic oral mucosa. Given that underlying tissue fibrosis can distort the fluorescence intensity of premalignant or malignant lesions, we further compared the ratios of $A_{460\pm10\,nm}/A_{380\pm10\,nm}$ among NOM and EH, ED, or SCC lesions on OSF mucosa. Figure 5 shows the average normalized fluorescence spectra obtained from

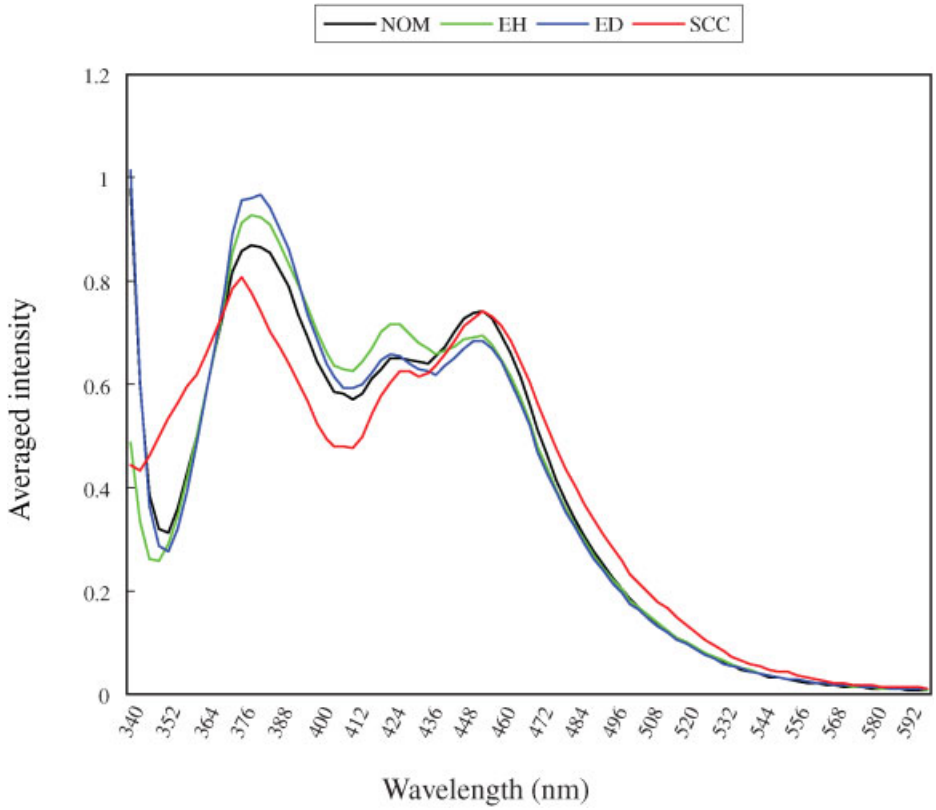

Fig. 5. Normalized averaged fluorescence emission spectra obtained from normal oral mucosa of healthy volunteer (NOM, n = 15) and OSF patients with epithelial hyperkeratosis (EH, n = 32), epithelial dysplasia (ED, n = 12), and squamous cell carcinoma (SCC, n = 7). Fluorescence intensities are reported in calibrated units.

TABLE 2. ANOVA Test for Mean Ratios of $A_{460 \pm 10\ nm}/A_{380 \pm 10\ nm}$ of NOM and EH or ED Lesions on Fibrotic Tissues

	ANOVA					
Variation source	SS	DOF	MS	F	*P* value	Threshold
Between groups	0.022668	2	0.011334	0.240686	0.786912	3.164999
Within group	2.590023	55	0.047091		($P > 0.05$)	
Sum	2.612691	57				

No significant differences were shown among the three groups.

NOM, and oral lesions of EH, ED, and SCC in OSF patients at 330-nm excitation. As shown in Table 2, the ANOVA test showed no significant differences in the mean ratio among NOM and EH or ED lesions on fibrotic mucosa tissues ($P > 0.05$). This result suggests that autofluorescence spectroscopy might not be effective for the diagnosis of EH, ED, and SCC lesions in OSF patients.

DISCUSSION

It has been shown that autofluorescence spectroscopy is associated with the structural matrix of tissues and cellular metabolic processes [5]. In addition, spontaneous porphyrin-like autofluorescence has also been noted on the surface of tissues with bacterial inhabiting in the absence of exogenously applied hematoporphyrin derivative [17]. As the observed emissions of our studies occurred around the 380 nm and 460 nm, it is unlikely that the observed autofluorescence relates to the microbial synthesis of porphyrins at the examined tissues of patients. Previous studies have demonstrated that the emission band at 380–400 nm is mainly attributed to the presence of collagen, while that at 440–460 nm is mainly due to the presence of NADH [6,18,19]. Using NMBA-induced rat esophageal carcinogenesis model, Glasgold et al. [18] showed that the fluorophore responsible for the 390-nm emission peak exists in the subepithelial connective tissue (collagen) and that responsible for the 450-nm emission peak exists in the epithelium (NADH). In these regards, the differences in autofluorescence spectra of NOM, OSF, EH, ED, and SCC samples might be attributed to the differences of collagen and NADH content in these samples. OSF mucosa has increased deposition of collagen in the subepithelial connective tissue and the atrophic oral epithelium [20,21]. Therefore, it was easy to explain why OSF samples had a higher 380-nm emission peak and a lower 460-nm emission peak than NOM samples. Oral EH and ED lesions in this study had a more thickened, acanthotic or dysplastic epithelium than NOM samples. The thickened epithelium might contain more NADH and reduce more collagen-derived emission fluorescence than NOM. This further explained why the EH or ED lesions had a lower 380-nm emission peak and a higher 460-nm emission peak than NOM samples. In our SCC samples, cancer cells proliferated outward and inward, resulting in a more thickened cancer tissue, which might contain more NADH, reduce more excitation light reaching the underlying collagen layer, and filter out more collagen-derived emission fluorescence than EH and ED samples. Moreover, only little stromal connective tissue (collagen) was found among oral cancer nests. These resulted in a much lower 380-nm emission peak and a much higher 460-nm emission peak for oral SCC lesions than those for EH and ED lesions.

When the oral EH, ED, and SCC lesions occurred in OSF patients, as shown in Figure 3B, the underlying tissue fibrosis resulted in a greater intensity of the 380-nm emission peak than the corresponding lesions in non-OSF patients (Fig. 3A). In addition, EH, ED, and SCC lesions on OSF mucosa contained a more atrophic lesional epithelium or cancer tissue due to the underlying tissue fibrosis. These atrophic epithelial or cancer tissues might contain less amount of NADH and thus had a lower 460-nm emission peak than the corresponding lesions in non-OSF patients. In Taiwan, oral premalignant and malignant lesions are commonly found in OSF patients and AQ-chewing habit prevails in patients with oral premalignant and malignant lesions [22]. As AQ-chewing habit may cause obscure to different degrees of fibrosis in the oral mucosa, autofluorescence spectra measured from premalignant, malignant and their surrounding normal tissues in AQ-chewers or OSF patients may be distorted due to the presence of underlying tissue fibrosis. This might explain why there was a considerable overlap in the ratios of $A_{460 \pm 10\ nm}/A_{380 \pm 10\ nm}$ between EH, ED, or SCC lesions and their normal tissues from the contralateral site of lesions in individual AQ-chewing patients. In addition, this also explained why we could not differentiate EH from ED lesions in AQ-chewing patients using autofluorescence spectroscopy.

This study represented the first to assess the spectral characteristics of fibrotic oral mucosa in OSF patients. Because underlying tissue fibrosis significantly affected the accuracy of autofluorescence diagnosis of oral premalignant and malignant lesions in OSF patients, we conclude that autofluorescence spectroscopy is a good technique for diagnosis of EH, ED, and SCC lesions in non-OSF patients but not in OSF patients.

REFERENCES

1. Ko YC, Chiang TA, Chang SJ, Hsiehn SF. Prevalence of betal quid chewing habit in Taiwan and related sociodemographic factors. J Oral Pathol Med 1992;21:261–264.
2. Kwan HW. A statistical study on oral carcinomas in Taiwan with emphasis on the relationship with betel nut chewing: A preliminary report. J Formosan Med Assoc 1976;75:497–505.
3. Huang JS, Kok SH, Kuo YS. Oral cancers in Taiwan: Review of the literature. Chinese J Oral Maxillofacial Surg 1994;5: 13–22.

4. Garfinkel L. Cancer statistics and trends. In: Holleb AI, Fink DJ, Murphy GP, editors. American Cancer Society Textbook of Clinical Oncology. Atlanta, GA: American Cancer Society; 1991. pp 1–6.
5. Richards-Kortum R, Sevick-Muraca E. Quantitative optical spectroscopy for tissue diagnosis. Annu Rev Phys Chem 1996;47:555–606.
6. Hung J, Lam S, LeRiche JC, Palcic B. Autofluorescence of normal and malignant bronchial tissue. Lasers Surg Med 1991;11:99–105.
7. Schomacker KT, Fusoli JK, Compton CC, Flotte TJ, Richter JM, Nishioka NS, Deutsch TF. Ultraviolet laser-induced fluorescence of colonic tissue: Basic biology and diagnosis potential. Lasers Surg Med 1992;12:63–78.
8. Ramanujam M, Mitchell MF, Mahadevan A, Warren S, Thomsen S, Silva E, Richards-Kortum R. In vivo diagnosis of cervical intraepithelial neoplasia using 337-nm-excited laser-induced fluorescence. Proc Natl Acad Sci USA 1994;91: 10193–10197.
9. Schantz SP, Kolli V, Savage HE, Yu G, Shah JP, Harris DE, Katz A, Alfano RR, Huvos AG. In vivo native cellular fluorescence and histological characteristics of head and neck cancer. Clin Cancer Res 1998;4:1177–1182.
10. Gillenwater A, Jacob R, Ganeshappa R, Kemp B, El-Naggar AK, Palmer JL, Clayman G, Mitchell MF, Richards-Kortum R. Noninvasive diagnosis of oral neoplasia based on fluorescence spectroscopy and native tissue autofluorescence. Arch Otolaryngol Head Neck Surg 1998;124:1251–1258.
11. Chen CT, Wang CY, Kuo YS, Chiang HH, Chow SN, Chiang CP. Light-induced fluorescence spectroscopy: A potential diagnostic tool for oral neoplasia. Proc Natl Sci Council ROC-Life Science 1996;20:123–130.
12. Chen CT, Chiang HH, Chow SN, Wang CY, Lee YS, Tsai JC, Chiang CP. Autofluorescence in normal and malignant human oral tissues and in DMBA-induced hamster buccal pouch carcinogenesis. J Oral Pathol Med 1998;27: 470–474.
13. Mahadevan A, Mitchell MF, Silva E, Thomsen S, Richards-Kortum RR. Study of the fluorescence properties of normal and neoplastic human cervical tissue. Lasers Surg Med 1993;13:647–655.
14. Eker C, Rydell R, Svanberg K, Andersson-Engels S. Multivariate analysis of laryngeal fluorescence spectra recorded in vivo. Lasers Surg Med 2001;28:259–266.
15. Hwang CY, editor. Multivariate analysis: An introduction. 5th edn. Taipei: Institute of Chinese Economy and Business; 1995. pp 20–23.
16. Albert A, Harris EK, editors. Multivariate interpretation of clinical laboratory data. USA: Marcel Dekker, Inc.; 1997. pp 76–82.
17. Harris DM, Werkhaven J. Endogenous porphyrin fluorescence in tumors. Lasers Surg Med 1987;7:467–472.
18. Glasgold R, Glasgold M, Savage H, Pinto J, Alfano R, Schantz S. Tissue autofluorescence as an intermediate endpoint in NMBA-induced esophageal carcinogenesis. Cancer Lett 1994;82:33–41.
19. Bottiroli G, Groce AC, Locatelli D, Marchesini R, Pignoli E, Tomatis S, Cuzzoni C, Dipalma S, Dalfante M, Spinelli P. Natural fluorescence of normal and neoplastic human colon: A comprehensive "ex vivo" study. Lasers Surg Med 1995; 16:48–60.
20. Kuttan R, Donnely PV, Di Ferrante N. Collagen treated with (+)-catechin becomes resistant to the action of mammalian collagenase. Experientia 1981;37:221–223.
21. Scutt A, Meghji S, Canniff JP, Harvey W. Stabilisation of collagen by betel nut polyphenols as a mechanism in oral submucous fibrosis. Experientia 1987;43:391–393.
22. Ma RH, Tsai CC, Shieh TY. Increased lysyl oxidase activity in fibroblasts cultured from oral submucous fibrosis associated with betel nut chewing in Taiwan. J Oral Pathol Med 1995; 24:407–412.